Supporting Information

Easily Accessible Polycyclic Amines that Inhibit the Wild-Type and Amantadine-Resistant Mutants of the M2 Channel of Influenza A Virus

Matias Rey-Carrizo,[ǂ] Marta Barniol-Xicota,[ǂ] Chunlong Ma,[#,§] Marta Frigolé-Vivas,[ǂ] Eva Torres,[ǂ] Lieve Naesens,[⊥] Salomé Llabrés,[Δ] Jordi Juárez-Jiménez,[Δ] Francisco J. Luque,[Δ] William F. DeGrado,[†] Robert A. Lamb,[§,∫] Lawrence H. Pinto,[#] Santiago Vázquez[ǂ]*

Table of contents

Elemental analysis data:

Compound	**Molecular Formula**	**Calculated**				**Found**			
		C	H	N	X	C	H	N	X
4·HCl	$C_{11}H_{15}N$·HCl	66.83	8.16	7.08	19.93	66.55	8.13	7.00	17.81
6·HCl·0.33H_2O	$C_{11}H_{17}N$·HCl·0.33H_2O	64.24	9.14	6.81	17.24	64.43	8.96	6.54	17.55
8·2.15HCl·H_2O	$C_{16}H_{24}N_2$·2.15HCl·H_2O	56.39	8.33	8.22	22.37	56.39	8.33	8.42	22.37
9·2HCl·0.5H_2O	$C_{16}H_{26}N_2$·2HCl·0.5H_2O	58.53	8.90	8.53	21.60	58.57	8.67	8.48	21.53
5·HCl·0.25H_2O	$C_{12}H_{17}N_3$·HCl·0.25H_2O	59.01	7.63	17.20	14.51	59.03	7.62	17.45	14.57
7·HCl·0.33H_2O	$C_{12}H_{19}N_3$·HCl·0.33H_2O	58.17	8.41	16.96	14.31	58.17	8.23	17.09	14.58
11·HCl·0.33H_2O	$C_{12}H_{15}N$·HCl·0.33H_2O	66.83	7.79	6.49	16.44	66.65	7.82	6.51	16.10
12·HCl·0.5H_2O	$C_{12}H_{19}N$·HCl·0.5H_2O	64.70	9.50	6.29	15.92	64.85	9.72	6.27	15.78
13·1.1HCl	$C_{13}H_{17}N_3$·1.1HCl	61.14	7.14	16.45	nd	61.40	7.48	16.47	nd
14·HCl	$C_{13}H_{21}N_3$·HCl	61.04	8.67	16.43	13.86	60.99	8.96	16.15	13.62
18·HCl·0.6H_2O	$C_{16}H_{25}N$·HCl·0.6 H_2O	68.70	9.84	5.01	nd	68.98	9.70	4.79	nd
19·1.1HCl·0.6H_2O	$C_{17}H_{27}N_3$·1.1HCl·0.6H_2O	62.75	9.11	12.91	11.98	62.47	8.84	13.06	11.72

Figure S1. Selected geometrical parameters (distances in Å; tilt angle in degrees) for the binding of compound **18** to the wt M2 channel along the trajectories sampled for the three 50 ns MD replicas.
Left: Distance from the amine N to the His37 plane and tilt angle (defined as the angle between amine N, COM of ligand, and COM of His37 Cα atoms). Right: distances from the COM of ligand to the plane formed by tetrads of residues along the pore.

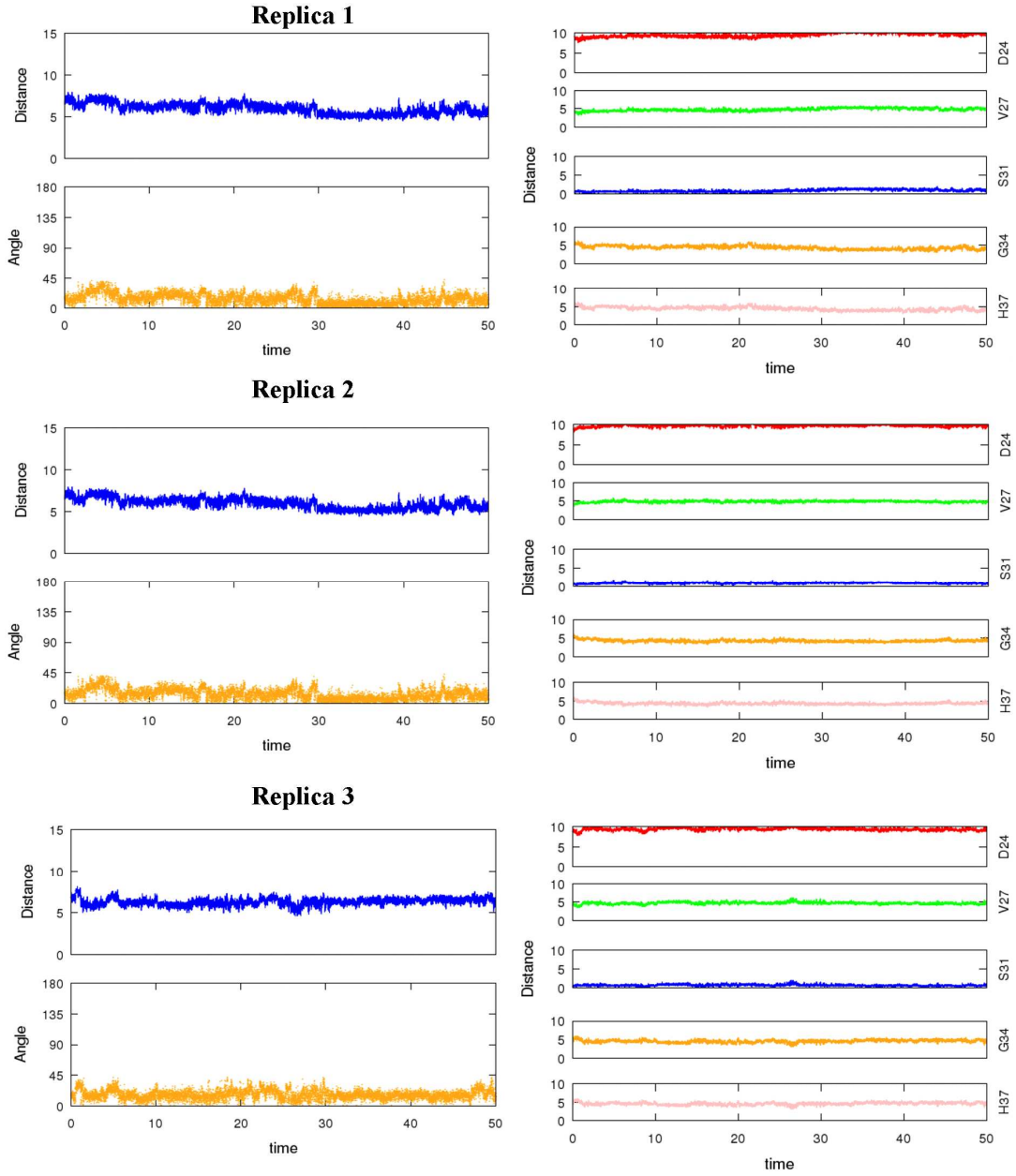

Replicas 1-3 show a stable arrangement of compound **18** in the pore, which is characterized by a distance from the amine nitrogen to the plane formed by the His37 residues close to 6.1 Å, and a tilt angle close to 16 degrees. Finally, the COM of the ligand is located close to the plane defined by the tetrad of Ser31 residues.

Figure S2. Selected geometrical parameters (distances in Å; tilt angle in degrees) for the binding of Amt to the wt M2 channel along the trajectories sampled for the three 50 ns MD replicas.
Left: Distance from the amine N to the His37 plane and tilt angle (defined as the angle between amine N, COM of ligand, and COM of His37 Cα atoms). Right: distances from the COM of ligand to the plane formed by tetrads of residues along the pore.

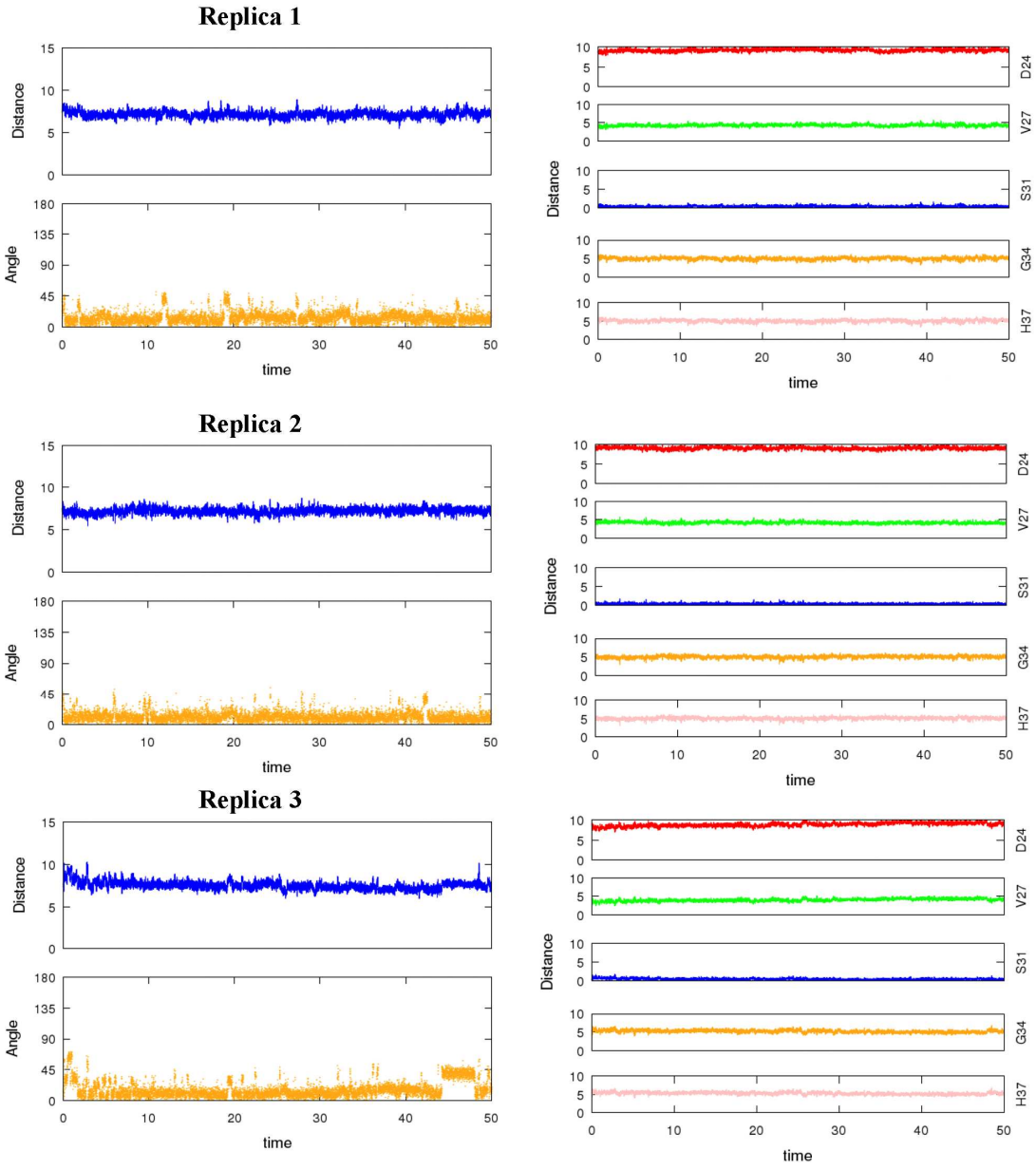

Replicas 1-3 show a stable arrangement of Amt in the pore, which is characterized by a distance from the amine nitrogen to the plane formed by the His37 residues close to 6.1 Å, and a tilt angle close to 16 degrees. Finally, the COM of the ligand is located close to the plane defined by the tetrad of Ser31 residues.

Figure S3. Selected geometrical parameters (distances in Å; tilt angle in degrees) for the binding of compound **18** to the V27A variant of the M2 channel along the trajectories sampled for the three 50 ns MD replicas.
Left: Distance from the amine N to the His37 plane and tilt angle (defined as the angle between amine N, COM of ligand, and COM of His37 Cα atoms). Right: distances from the COM of ligand to the plane formed by tetrads of residues along the pore.

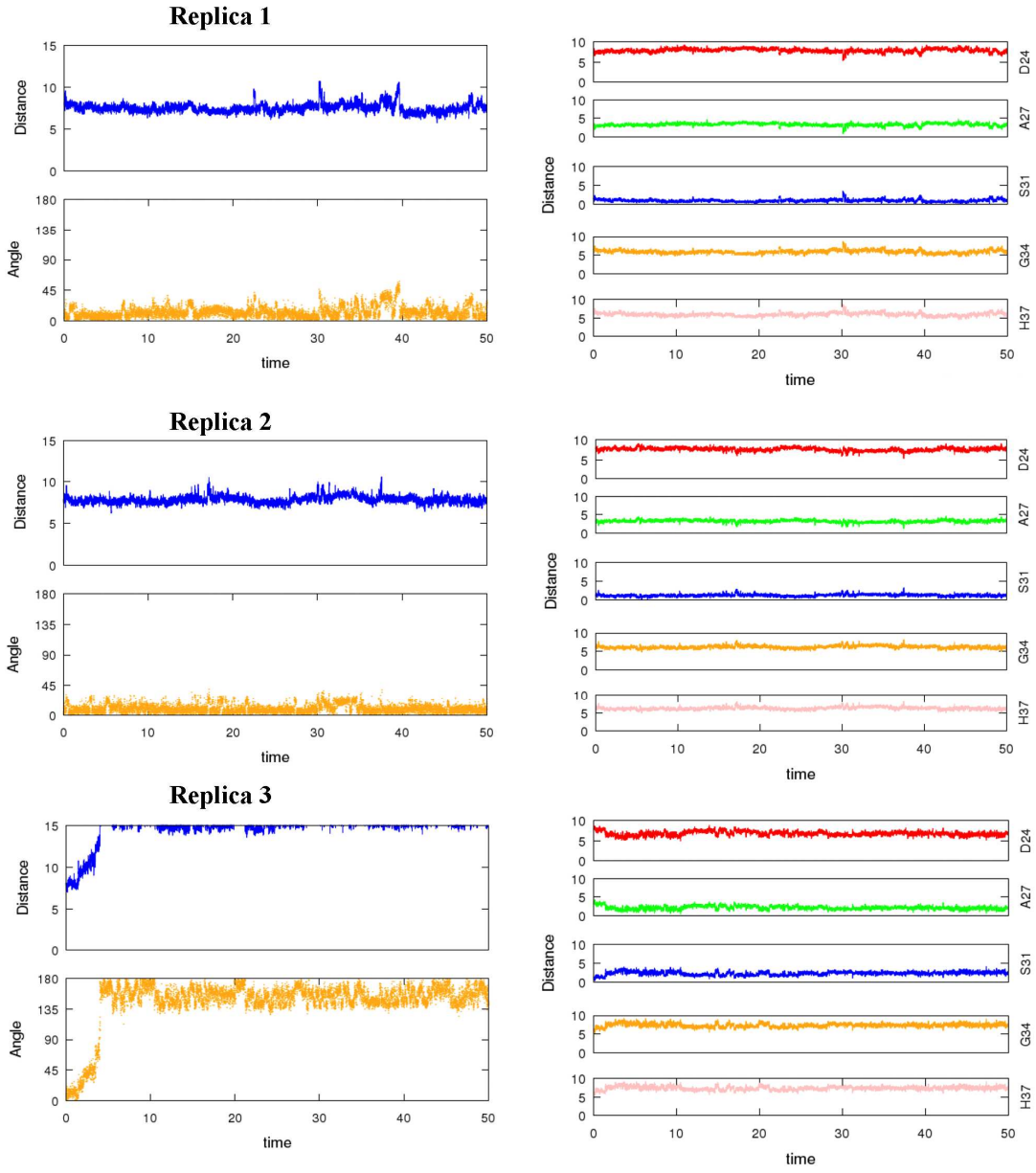

Replicas 1 and 2 exhibit a common arrangement of compound **18** in the pore, which is characterized by a distance from the amine nitrogen to the plane formed by the His37 residues close to 7.5 Å, and a tilt angle close to 12 degrees. Moreover, the COM of the ligand is shifted 1.1 Å from the plane formed by the tetrad of Ser31 residues.
Replica 3 differs due to the rearrangement of the inhibitor in the pore, as the amine nitrogen is now pointing toward the entrance to the channel. Thus, the distance from the amine nitrogen to the plane formed by the His37 residues is close to 15 Å, and the tilt

angle is close to 145 degrees. Finally, the COM of the ligand is further displaced toward the mouth of the channel, as the distance of the ligand COM to the plane formed by the tetrad of Ser31 residues is 2.3 Å.

Figure S4. Selected geometrical parameters (distances in Å; tilt angle in degrees) for the binding of Amt to the V27A variant of the M2 channel along the trajectories sampled for the three 50 ns MD replicas.
Left: Distance from the amine N to the His37 plane and tilt angle (defined as the angle between amine N, COM of ligand, and COM of His37 Cα atoms). Right: distances from the COM of ligand to the plane formed by tetrads of residues along the pore.

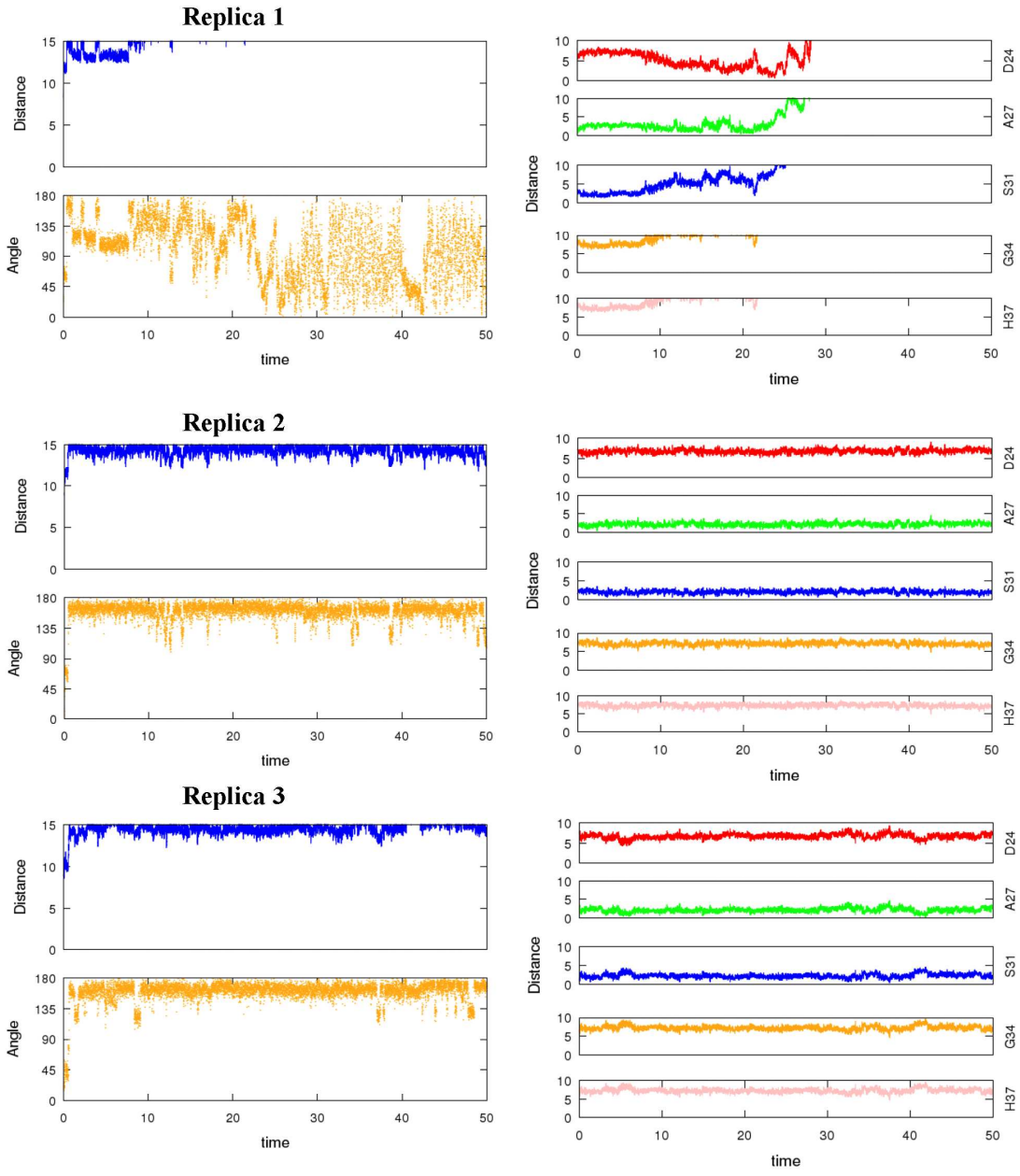

Replicas 2 and 3 exhibit a common arrangement of Amt in the pore, which is characterized by a distance from the amine nitrogen to the plane formed by the His37 residues close to 14.5 Å, and a tilt angle close to 159 degrees. Therefore, the arrangement of Amt is opposite to that found in the wt M2 channel. Furthermore, the COM of the ligand is located between the planes defined by tetrads of Val27 and Ser31 residues, as the distance to these planes is 2.2 and 2.1 Å, respectively.

Replica 1 exhibits a different behaviour, because the inhibitor was released from the pore to the bulk solution after the first 10 ns of the trajectory

Figure S5. Cross-diagonals between transmembrane helices in the M2 channel.

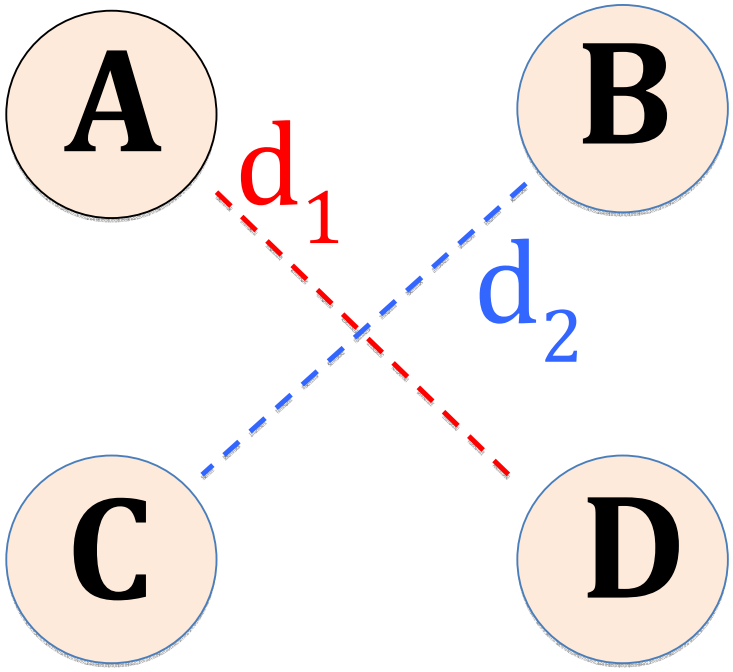

Figure S6. (A) Superposition of the NMR-derived structure obtained for the complex between the S31N channel and the 5-thienyl isoxazole derivative (PDB entry 2LY0; orange) and a representative snapshot of the complex between wt M2 channel and compound **18** (green). (B) Representation of the relative alignment of the 5-thienyl isoxazole derivative and compound 18 bound to S31N and wt channels, respectively.

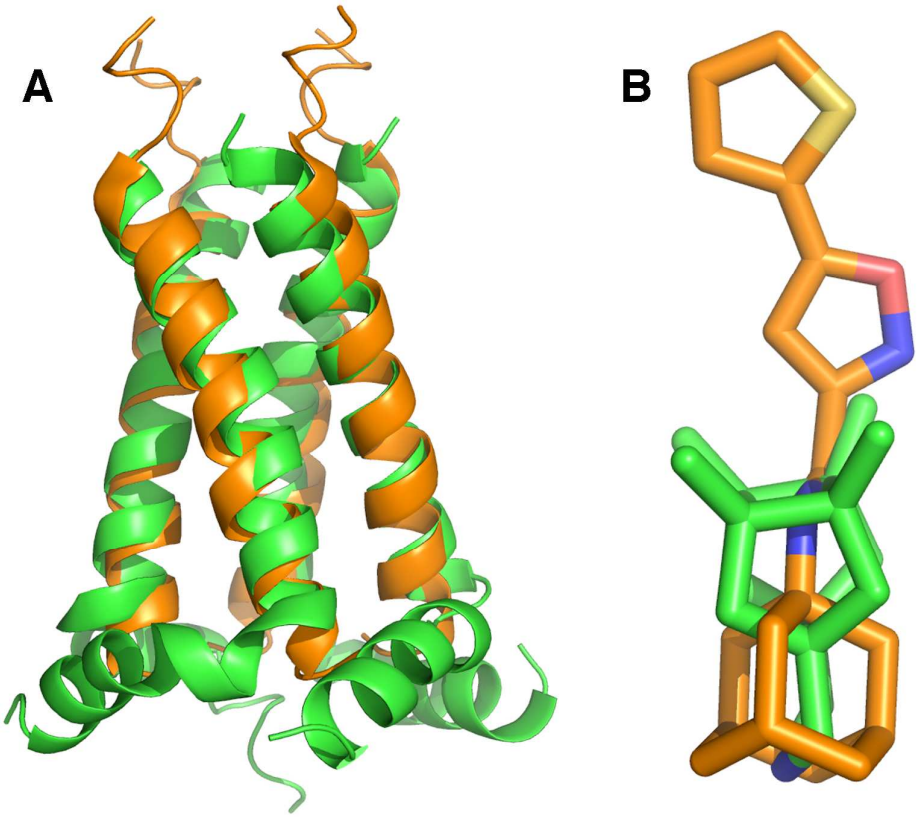

Table S1. Root-mean square deviations (Å) between the backbone atoms of the transmembrane helices of the wt M2 channel and its V27A variant in both apo and holo forms. Values determined for the averaged structure sampled in the last 10 ns of the trajectories.

Wild type		Holo(Amt)			Holo(**18**)		
		1	*2*	*3*	*1*	*2*	*3*
Apo		1.4	1.7	1.3	1.5	1.6	1.3
Holo(Amt)	*1*		1.2	1.0	1.2	1.6	1.2
	2			1.4	1.1	1.6	1.5
	3				1.2	1.4	1.2
Holo(**18**)	*1*					1.2	1.2
	2						1.4

V27A		Holo(Amt)			Holo(**18**)		
		1	*2*	*3*	*1*	*2*	*3*
Apo		1.5	1.3	1.8	1.5	1.3	1.4
Holo(Amt)	*1*		1.8	1.3	1.7	1.7	1.8
	2			1.8	1.2	1.2	1.4
	3				1.5	1.7	1.9
Holo(**18**)	*1*					1.3	1.4
	2						1.4